JES
Journal of Engineering Sciences

Vol 10, Issue 9, Sept /2019
ISSN NO:0377-9254

FUZZY BASED GAN BASED TRANSFORMER-LESS MICROINVERTER WITH COUPLED INDUCTOR INTERLEAVED BOOST AND HALF BRIDGE VOLTAGE SWING INVERTER

[1] P.SANJEEVA RAYUDU, [2]G.VEERA SANKARA REDDY, [3]M.NAVEEN BABU
[1]PG Student, [2,3]Asst.Professor
Department Of Electrical Electronics Engneering
TADIPATRI ENGNEERING COLLEGE, TADIPATRI

ABSTRACT

Due to their plug and play feature, easy installation, and higher power yield under partial shading conditions, microinverters have gained popularity in the roof-top-PV market. This paper explores a converter system for the transfomer-less microinverter with coupled inductor based interleaved boost as the dc-dc stage and half bridge voltage swing (HBVS) inverter with indction motor by using fuzzy logic as the dc-ac stage. The dc-dc stage is capable of offering high gain with a flexible choice of turns ratio of the coupled inductor but simultaneously maintaining a reduced voltage stress on the main switch. The HBVS inverter has the advantages of reduced capacitor requirement for 120 Hz power decoupling and being half-bridge derived, minimized capacitive-coupled common-mode ground currents. A 300 W GaN based inverter prototype with 30 V nominal dc input and 120 V, 60 Hz nominal ac output and operating at switching frequency of 200/100 kHz has been developed .

I. INTRODUCTION

Photovoltaic (PV) inverters form the backbone of both utility and residential grid-connected PV systems. Recently, in such applications micro inverters are increasingly grabbing more market share due to its easy installation, plug and play concept, and higher power yield under partial shading condition. As they are directly connected to each of the PV panel, typically the input voltage for such inverters spans from 30 to 40 V, whereas, to interface to the grid the ac output voltage needs to be 120 V/ 230 V RMS. This necessitates a high voltage boost for interfacing a PV panel to the grid. Thus most of the commercialized micro inverters are implemented with high frequency transformer isolation providing higher voltage step-up through the turns ratio accommodation as is done in . However, transformer-less versions are preferred because of their advantages in higher efficiency, reduced volume, and lower cost with the removal of lossy and bulky transformer. Authors in have proposed non-isolated high gain boost converters which are also suitable to implement as the high gain stage of transformer-less microinverter applications. The other two challenges encountered by any transformer-less microinverters are similar to that of any PV string inverters implemented without isolation. These include the mitigation of the capacitively coupled ground current arising from the parasitic capacitance between the PV panel and grid neutral and similar to any other single phase rectifiers and inverters, the need to support double line frequency power decoupling with reliable and efficient film capacitors. In this paper, a converter system for the transfomerless microinverter with coupled inductor based interleaved boost as the dc-dc stage and half bridge voltage swing (HBVS) inverter as the dc-ac stage is proposed. The dc-dc stage has two interleaved phases and is capable of offering high gain with a flexible choice of turns ratio of the coupled inductor but simultaneously maintaining a reduced voltage stress on the main switches of both the phases. Additionally, the inductor current is interleaved, reducing the equivalent ripple on the converter input current and the inductor core loss and high frequency copper loss. The HBVS inverter [16]–[19] has the advantages of connecting the PV negative terminal to the grid neutral through line frequency varying half bridge capacitor, thereby eliminating the capacitive-coupled common-mode ground currents, critical for all transformer-less PV inverters. Also through sinusoidal variation of the half bridge capacitor voltage along with a limited ripple on the dclink, the decoupling capacitor is reduced allowing an all-film capacitor implementation. The rest of the paper is organized as follows. Section II gives a detail of the basic converter operating principles of both the high gain dc-dc stage and half bridge derived dc-ac stage. Passive and active component details along with controller design are presented in the following Section III. Detailed experimental results for a 300 W hardware prototype designed for microinverter application with GaN devices are also provided here.

Journal of Engineering Sciences

II. LITERATURE SURVEY

"A high voltage-gain LLC micro-converter with high efficiency in wide input range for PV applications,"

This paper proposes a novel high voltage-gain LLC micro-converter for PV applications. The converter has simple structure and minimum components with low cost. It can realize high voltage gain based on the voltage doubler rectifier with the optimal turns ratio. The main power switches can achieve ZVS and the output diodes can realize ZCS in wide input and load range. By utilizing the voltage doubler in the secondary side, the voltage stress over the output diodes can be reduced by half compared to the conventional center-tapped full-wave rectifier. A 24-48 V input, 380 V output and 200W prototype was built to verify the benefits of the proposed converter. The achieved efficiency of the converter peaks at 96.6% and the CEC weighted efficiency reaches 95.4% .

Modelling and control design of paralleled DC–DC switching converters

Power electronic systems are widely used today to provide power processing for applications ranging from computing and communications to medical electronics, appliance control, transportation, and high-power transmission. The associated power levels range from milli watts to megawatts. These systems typically involve switching circuits composed of semiconductor switches such as thyristors, MOSFETs, and diodes, along with passive elements such as inductors, capacitors, and resistors, and integrated circuits for control. Application of Kalman filters in model-based fault diagnosis of a DC–DC boost converter

A time-averaging model was used with the Kalman filters to generate residual signals. Multiple signature faults were developed in fault scenarios to identify critical variations in the elements of a power converter using the adaptive estimation technique. Results show a very precise and accurate fault diagnosis of signature faults. The fault diagnosis shows a high performance in transients and against noise in the circuit. Parameter estimation of a dc/dc buck converter using a continuous time model

A novel online technique for estimating the parameters of a DC/DC buck converter through a continuous time model is proposed. Standard least mean squares algorithm is applied among other formulations, taking into account only the non conduction state during a single switching cycle. The problem of derivative calculation of the needed voltage and current signals is solved by polynomial interpolation. An online technique for estimating the parameters of passive components in non-isolated DC/DC converters

a novel online technique used for estimating the parameters of passive components in non-isolated DC/DC converters is presented. The technique is implemented for the boost and buck-boost converters, operating both in continuous current mode (CCM) and discontinuous current mode (DCM). The technique is based on the sampling of the MOSFET gate signal, inductor current and load voltage, which is followed by the processing of the acquired data through different ways such as the least mean squares algorithm. The knowledge of these passive components parameters may be used in the fault diagnosis of such converters. Results obtained from simulations are presented, followed by experimental results in which the inductance, capacitance, load resistor and ESR of the capacitor are estimated, in order to validate the proposed technique.

III. PHOTOVOLTAIC INVERTER

The basic block diagram of grid connected PV power generation system is shown in Fig.

The PV power generation system consists of following major blocks:

1. PV unit
2. Inverter
3. Grid
4. MPPT

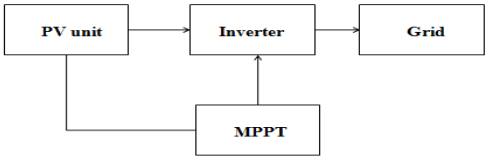

Fig.1 Schematic diagram of PV system

1. PV unit : A PV unit consists of number of PV cells that converts the energy of light directly into electricity (DC) using photovoltaic effect.
2. Inverter : Inverter is used to convert DC output of PV unit to AC power.
3. Grid : The output power of inverter is given to the nearby electrical grid for the power generation.
4. MPPT : In order to utilize the maximum power produced by the PV modules, the power conversion equipment has to be equipped with a maximum power point tracker (MPPT). It is a device which tracks the voltage at where the maximum power is utilized at all times.

Journal of Engineering Sciences
Vol 10, Issue 9, Sept /2019
ISSN NO:0377-9254

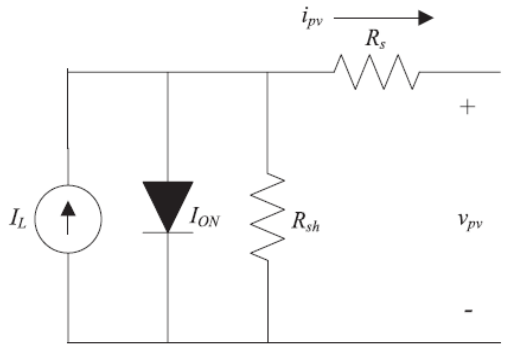

Fig.2 Equivalent circuit diagram of the PV cell

Perturb and Observe algorithm

At present, the most popular MPPT method in the PV systems is perturb and observe. In this method, a small perturbation is injected to the system and if the output power increases, a perturbation with the same direction will be injected to the system and if the output power decreases, the next injected perturbation will be in the opposite direction.

The Perturb and observe algorithm operates by periodically perturbing (i.e. incrementing or decrementing) the array terminal voltage and comparing the PV output power with that of the previous perturbation cycle.

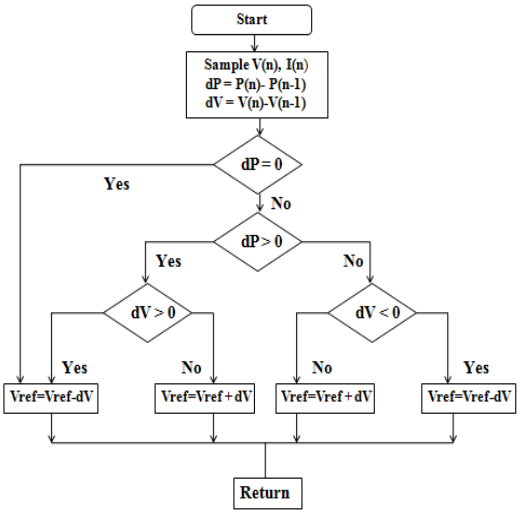

Fig.3 Flow chart of perturb and observe

IV.FUZZY

In recent years, the number and variety of applications of fuzzy logic have increased significantly. The applications range from consumer products such as cameras, camcorders, washing machines, and microwave ovens to industrial process control, medical instrumentation, decision support systems, and portfolio selection. To understand why use of fuzzy logic has grown, you must first understand what is meant by fuzzy logic.

Fuzzy logic has two different meanings. In a narrow sense, fuzzy logic i s a logical system, which is an extension of multivalve logic. However, in a wider sense fuzzy logic (FL) is almost synonymous with the theory of fuzzy sets, a theory which relates to classes of objects with un sharp boundaries in which membership is a matter of degree. In this perspective, fuzzy logic in its narrow sense is a branch of FL. Even in its more narrow definition, fuzzy logic differs both in concept and substance from traditional multivalve logical systems.

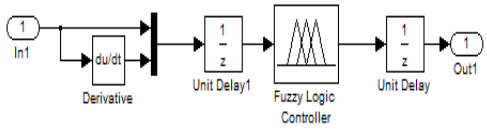

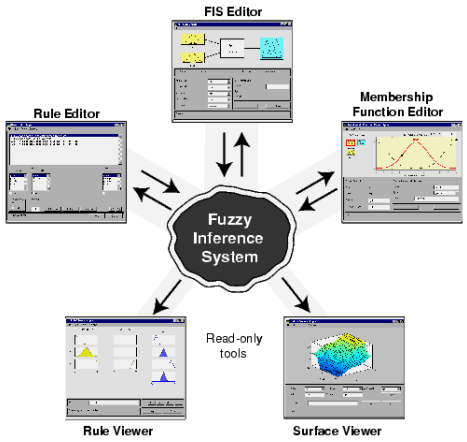

Fig.4 Fuzzy interference system &
The primary GUI tools of the fuzzy logic toolbox

V.INDUCTION MOTOR

An **induction motor** or **asynchronous motor** is an AC electric motor in which the electric current in the rotor needed to produce torque is obtained by electromagnetic induction from the magnetic field of the stator winding.[1] An induction motor can therefore be made without electrical connections to the rotor.[a] An induction motor's rotor can be either wound type or squirrel-cage type.

Three-phase squirrel-cage induction motors are widely used as industrial drives because they are rugged, reliable and economical. Single-phase induction motors are used extensively for smaller loads, such as household appliances like fans. Although traditionally used in fixed-speed service, induction motors are increasingly being used with variable-frequency drives (VFDs) in variable-

speed service. VFDs offer especially important energy savings opportunities for existing and prospective induction motors in variable-torque centrifugal fan, pump and compressor load applications. Squirrel cage induction motors are very widely used in both fixed-speed and variable-frequency drive (VFD) applications.

VI.PI controller

The general block diagram of the PI speed controller is shown in Figure 2

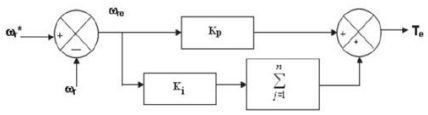

FIG. 2. Block diagram of PI speed controller.

The output

Of the speed controller (torque command) at *n*-th instant is expressed as follows:

$Te\,(n)=Te(n-1)+Kp\_\omega re(n)+Ki\omega re(n)$ (10)

Where *Te* (*n*) is the torque output of the controller at the *n*-th instant, and *Kp* and K*i* the

proportional and integral gain constants, respectively.

A limit of the torque command is imposed as

$$T_{e(n+1)}=\begin{cases} T_{e\max} & \text{for } T_{e(n+1)}\geq T_{e\max} \\ -T_{e\max} & \text{for } T_{e(n+1)}\leq -T_{e\max} \end{cases}$$

The gains of PI controller shown in (10) can be selected by many methods such as trial

and error method, Ziegler–Nichols method and evolutionary techniques-based searching. The

numerical values of these controller gains depend on the ratings of the motor.

VII.PROPOSED AND CONTROL DESIGN

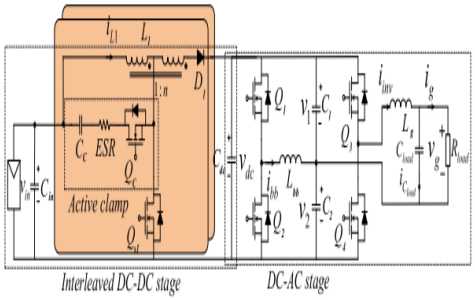

Fig. 1. Transformer-less microinverter topology in stand-alone mode with coupled inductor interleaved boost as dc-dc stage and half bridge voltage swing inverter as dc-ac stage.

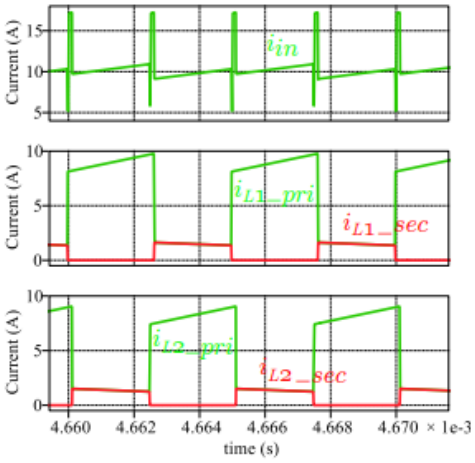

Fig. 2. Current waveforms for the ideal interleaved coupled inductor boost converter.

Fig. shows the coupled inductor based interleaved boost followed by HBVS inverter considered for the transformer-less microinverter application.

The high gain dc-dc stage is realized by coupled inductor with two interleaved phases, whereas, the dc-ac stage offers an active power decoupling approach with a large sinusoidal swing of the half bridge capacitors with a limited 120 Hz ripple on the dc-link to minimize the decoupling capacitor requirement. It also mitigates the capacitive ground current. Also the topological variation offers connecting the grid neutral directly to the PV negative terminal through half bridge capacitor, which mitigates the capacitive ground current. A. Coupled inductor interleaved boost Fig.6.1 shows the circuit schematic of the coupled inductor interleaved boost converter for providing high voltage gain. In the present application, two interleaved phases are considered to scale the power. They process power in parallel. Each phase is comprised of the active switch Qs, diode D, and coupled inductor L with turns ratio 1 : n as shown. The subscript ′1 ′ in Fig. 1 refers to the components in phase I. The similar components are repeated for phase gives the input current (iin) and primary and secondary side coupled inductor current for both the interleaved phases assuming ideal coupling under continuous conduction mode (CCM) condition. The converter gain (k) is a function of the coupled inductor turns ratio n as given in (1). k = Vo Vin = iL1 + iL2 io = 1 + nD 1 − D (1) The MOSFET and diode voltage stress of the main circuit are given in (2), which shows that the stress on the MOSFET (Vsw m) is significantly reduced, thus lower voltage rating switch with lower ON-resistance RDS ON (which almost varies proportionally with the square of the blocking-voltage) can be used, reducing the corresponding conduction loss. However, the diode

voltage stress (Vdiode m) is in fact higher than the conventional boost. But it would not affect the converter efficiency as the SiC diode forward voltage drop does not scale remarkably with the voltage rating and diode current is significantly lower than the main switch current. Vsw m = Vo + nVin 1 + n ; Vdiode m = Vo + nVin (2) For practical implementation (Fig.shows the coupled inductor of each phase) the primary and secondary windings of the coupled inductor would not be ideally coupled introducing leakage path in the switching circuit, voltage oscillation, and power dissipation. Thus an active clamp is used here to ensure the recycling of the leakage.

On the main switch. But this introduces an additional active switch, the associated gate driver circuitry, and corresponding loss in the driving circuit. Qc and Cc constitute the active clamp circuit for each phase. Qc is operated in complementary to Qs with appropriate dead-time. B. Half bridge voltage swing inverter The output from the dc-dc stage vdc gets connected to the HBVS inverter stage as its input. The dc-ac stage is comprised of a synchronous buck-boost stage followed by a half bridge inverter. The grid neutral is directly connected to the PV negative terminal through half bridge capacitor, which mitigates the capacitive ground current, a critical requirement for transformer-less PV inverters as discussed in Section I. The grid voltage and grid current at an arbitrary power factor cos θ, with the corresponding instantaneous grid power are given in (3). vg = Vg sin(ωt); ig = Ig sin(ωt + θ) Pg = VgIg 2 (cos θ − cos(2ωt + θ)) (3) As Pg has 2ω ripple component and power from PV is a pure dc, the instantaneous power from input is not equal to that of the output and energy storage element is required to ensure power decoupling i.e., instantaneous power balance. In this converter a large sinusoidal swing of the half-bridge capacitors v1 and v2 [expressions are given in (4] are allowed along with a limited double line frequency voltage ripple on the dc-link v3 [given in (5)] to address the power decoupling with a reduced capacitor value. v1 = v3 2 +A sin(ωt+ζ); v2 = v3 2 −A sin(ωt+ζ) (4) vdc = V + Vr sin(2ωt + θ) (5) where, 2A is the allowed peak-peak ripple of the halfbridge capacitor voltages, ζ is their phase shift relative to the grid voltage, V is the dc-link average voltage, and Vr is the amplitude of dc-link ripple voltage. The ripple power Pi supported by any capacitor Ci is given in (6). Pi = 1 2 d dt Civ 2 i (6) Using (6), the total ripple power supported by all the three capacitors C1, C2, and Cdc can be computed [20] which is Pt = P1 + P2 + Pdc. By comparing the magnitude and phase of 2ωt terms in Pg and Pt, the condition for double line frequency power decoupling as given in (7) is obtained. V Vr(2Cdc + C) + CA2 = VgIg 2ω = Sg ω ζ = π 4 + θ 2 (7) Further, in order to regulate the grid current and voltage without distortion, the condition given in (8) needs to be satisfied instantaneously ensuring that the converter is not over-modulated at any operating interval. (v1 > vg if vg ≥ 0 v2 > |vg| if vg < 0)

VIII.SIMULATION DIAGRAMS

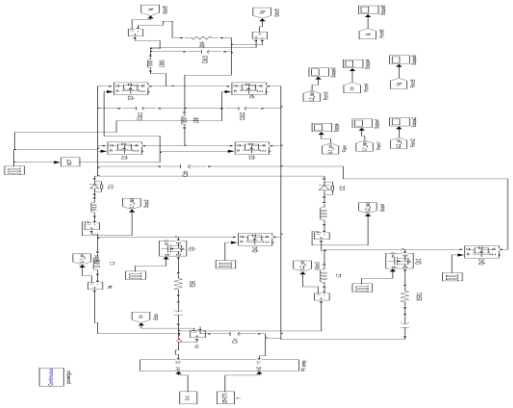

Fuzzy with induction daigram

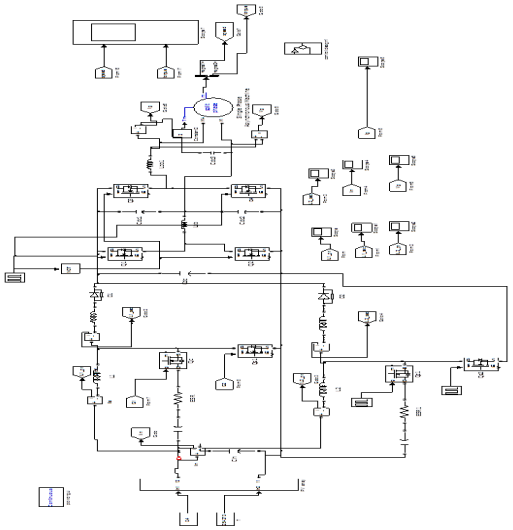

IX.CONCLUSION

The paper discusses a transformer-less micro inverter topology. The coupled inductor based interleaved boost dc-dc stage is capable of offering high gain with a flexible choice of turns ratio of the coupled inductor but simultaneously maintaining a reduced voltage stress on the main switch. The HBVS inverter dc-ac stage has the advantages of reduced capacitor requirement for 120 Hz power decoupling and being half-bridge derived, minimized capacitive-coupled common-mode ground currents. Experimental results are provided to validate its operation.

REFERENCES

[1] H. D. Gui, Z. Zhang, X. F. He, and Y. F. Liu, "A high voltage-gain LLC micro-converter with high efficiency in wide input range for PV applications," in 2014 IEEE Applied Power Electronics Conference and Exposition - APEC 2014, March 2014, pp. 637–642.

[2] J. Roy, Y. Xia, and R. Ayyanar, "Gan based transformer-less microinverter with extended-duty-ratio boost and doubly grounded voltage swing inverter," in 2017 IEEE Applied Power Electronics Conference and Exposition (APEC), March 2017, pp. 2970–2976.

[3] M. Kasper, M. Ritz, D. Bortis, and J. W. Kolar, "PV panelintegrated high step-up high efficiency isolated GaN DC-DC boost converter," in Telecommunications Energy Conference 'Smart Power and Efficiency' (INTELEC), Proceedings of 2013 35th International, Oct 2013, pp. 1–7.

[4] N. Sukesh, M. Pahlevaninezhad, and P. K. Jain, "Analysis and implementation of a single-stage flyback PV microinverter with soft switching," IEEE Transactions on Industrial Electronics, vol. 61, no. 4, pp. 1819–1833, April 2014.

[5] R. K. Surapaneni and A. K. Rathore, "A single-stage ccm zeta microinverter for solar photovoltaic ac module," IEEE Journal of Emerging and Selected Topics in Power Electronics, vol. 3, no. 4, pp. 892–900, Dec 2015.

[6] J. Roy and R. Ayyanar, "Seamless transition of the operating zones for the extended-duty-ratio boost converter," in 2017 IEEE Energy Conversion Congress and Exposition (ECCE), Oct 2017, pp. 4920–4926.

[7] L. H. S. C. Barreto, P. P. Praa, D. S. Oliveira, and R. N. A. L. Silva, "High-voltage gain boost converter based on three-state commutation cell for battery charging using PV panels in a single conversion stage," IEEE Transactions on Power Electronics, vol. 29, no. 1, pp. 150–158, Jan 2014.

[8] J. Roy and R. Ayyanar, "Gan based high gain non-isolated dc-dc stage of microinverter with extended-duty-ratio boost," in 2016 IEEE Energy Conversion Congress and Exposition (ECCE), Sept 2016, pp. 1–8.

AUTHOR'S:

P.SANJEEVA RAYUDU

I Completed My B.Tech TadipatriEngneering College, Affiliated to JNTUA Ananthapuramu. Now he is pursing M.Tech in Power Electronics from Tadipatri Engneering College ,Affiliated to JNTUA Ananthapuramu, Andharapradesh.Area of interest Power Electronics.

Email Id:sanjeev225143@gmail.com

G.VEERA SANKARA REDDY

Received the Master Of Technology in Power System Control and Automation from Aurora's Technological & Research Institute ,Affiliated to JNTUH ,Hyderabad.B.Tech Degree from Vaagdevi Institute Of Technology & Science , Affiliated to JNTUA ,Ananthapuramu. Currently he is working as Asst.Professor in Tadipatri Engneering College in department of Electrical Electronics Engneering , Tadipatri ,Ananthapuramu ,Andharapradesh.Area of interest Power System Control and Automation.

Email Id:gvsr.269@gmail.com

M.NAVEEN BABU

Received the Master Of Technology in Elecrical Power System from Sri Krishnadevaraya Engneering College ,Gooty,JNTUA University,Ananthapuramu. B.Tech Degree from Madanapalle Institute Of Technology & Science ,Affiliated to JNTUA , Ananthapuramu.Curren tly he is working as Asst.Professor & HOD in Tadipatri Engneering College in department of Electrical Electronics Engneering , Tadipatri ,Ananthapuramu ,Andharapradesh.Area of interest Electrical Machines, Power System.

Email Id:naveenbabumidde@gmail.com

Journal of Engineering Sciences